ELSEVIER

Materials Characterization 57 (2006) 259–273

MATERIALS CHARACTERIZATION

3D reconstruction and characterization of polycrystalline microstructures using a FIB–SEM system

M.A. Groeber [a], B.K. Haley [b], M.D. Uchic [c], D.M. Dimiduk [c], S. Ghosh [d,*]

[a] Department of Materials Science and Engineering, The Ohio State University, Columbus, OH 43210, USA
[b] Department of Computer Science and Engineering, The Ohio State University, Columbus, OH 43210, USA
[c] Air Force Research Laboratory, Materials and Manufacturing Directorate, AFRL/MLLMD, Wright-Patterson AFB, OH 45433-7817, USA
[d] Department of Mechanical Engineering, The Ohio State University, Columbus, OH 43210, USA

Received 1 August 2005; accepted 31 January 2006

Abstract

A novel methodology is described in this paper which is a step towards three-dimensional representation of grain structures for microstructure characterization and processing microstructural data for subsequent computational analysis. It facilitates evaluation of stereological parameters of grain structures from a series of two-dimensional (2D) electron backscatter diffraction (EBSD) maps. Crystallographic orientation maps of consecutive serial sections of a micron-size specimen are collected in an automated manner using a dual-beam focused ion beam–scanning electron microscope (FIB–SEM) outfitted with an EBSD system. Analysis of the serial-sectioning data is accomplished using a special purpose software program called "Micro-Imager". Micro-Imager is able to output characterization parameters such as the distribution of grain size, number of neighboring grains, and grain orientation and misorientation for every 2D section. Some of these data can be compared with results from stereological exercises. Stacking the 2D statistical information obtained from the analysis of the serial-sectioning data provides a means to quantify the variability of grain structure in 3D.

Keywords: Microstructure; Morphology; Characterization; Focused-ion-beam

1. Introduction

The ability to characterize microstructure is an important tool for materials scientists, because it allows one to quantify microstructure–property relations and anticipate the capability of a material to perform in a given application as a function of process history. For example, it is well known that the grain-size of a material has a strong effect on mechanical properties; therefore, an accurate measure of the grain size distribution is desirable to predict material performance. Classical methods for characterizing microstructure usually involve viewing an image from a sectioned surface, where the area of interest is mechanically polished and viewed in an optical or scanning electron microscope (SEM) [1]. With adequate resolution in this image-analysis process, grain boundaries and second-phase particles can be delineated, and stereological methods can subsequently be used to infer three-dimensional (3D) statistical attributes from the 2D microstructural images.

However, there are a number of microstructural parameters such as feature connectivity, true feature

* Corresponding author.
E-mail address: ghosh.5@osu.edu (S. Ghosh).

1044-5803/$ - see front matter © 2006 Elsevier Inc. All rights reserved.
doi:10.1016/j.matchar.2006.01.019

size, and true feature shape that cannot be inferred from 2D sections [2]. For the example of grain-size measurements, a common stereological measurement, e.g. mean linear intercept, can be used to determine the average grain size, but only for certain assumptions of the grain morphology. By comparison, this measurement can be computed without any bias if a full 3D data set is available for the microstructure. In addition, many stereological parameters yield only average scalar quantities to describe microstructural features. Recognizing the fact that many properties (especially those associated with failure) require extreme values of the microstructure [3], it is evident that characterizing the full distribution of these features may be more appropriate for some predictive models [4,5].

The need to more completely characterize the 3D microstructure has led to the development of methods that allow one to directly obtain 3D microstructural data [6,7]. One methodology that has been successfully used to perform this task is serial sectioning [6,7]. However, this technique can be time-consuming and, if performed manually, can be prone to errors related to maintaining a constant sectioning thickness. This paper discusses a newly developed technique to characterize grain structure via serial sectioning utilizing a new type of electron microscope; a dual-beam focused ion beam–scanning electron microscope (FIB–SEM). This microscope is capable of highly localized micro-machining and ion imaging using the FIB column, and non-destructive high-resolution imaging or other analytical methods such as electron backscatter diffraction (EBSD) using the electron column. For this study, the FIB is used to serial-section specimens and the EBSD system is used to obtain an orientation map for each section. The dual-beam FIB–SEM shows great potential because it can be automated to perform this analysis without user interaction.

Focused ion beam or FIB has become very popular in the recent days and has been used by a number of researchers to serial section and visualize microstructure in 3D [8–15]. This technique has brought about a tremendous advancement in the ability to view the true 3D microstructure of metallic materials with complex microstructural morphology and crystallographic orientation. Many of the published literature (e.g. [8–15]) provide only "slice and view" data. Sample repositioning in these studies was generally performed manually. Most of these experiments conduct fine-scale sectioning using a single beam FIB. Sakamoto et al. [8] and Fraser et al. [14] have used dual-beam FIB–SEM techniques to acquire morphological data for microanalysis. Much of this study, while sufficient for 3D reconstruction and visualization, does not contain adequate quantitative orientation information or allow for a completely automated method for grain segmentation to be incorporated. Additionally, manual sectioning is simply not feasible, even with a FIB, when collecting a large-scale high-resolution 3D data, a necessary ingredient for high fidelity statistical characterization.

This paper presents three significant advancements over the previous work, through (i) automated sectioning and scanning, (ii) collecting orientation data on each section for providing quantitative 3D crystallographic data, and (iii) automated segmenting and characterizing microstructural features. Customized scripts are developed in this work to completely control the FIB–SEM system during the sectioning and EBSD collection. The collection of EBSD maps on every section yields a completely automated path to grain reconstruction and segmentation. In addition to visualization, this work introduces a new methodology for the collection of 3D

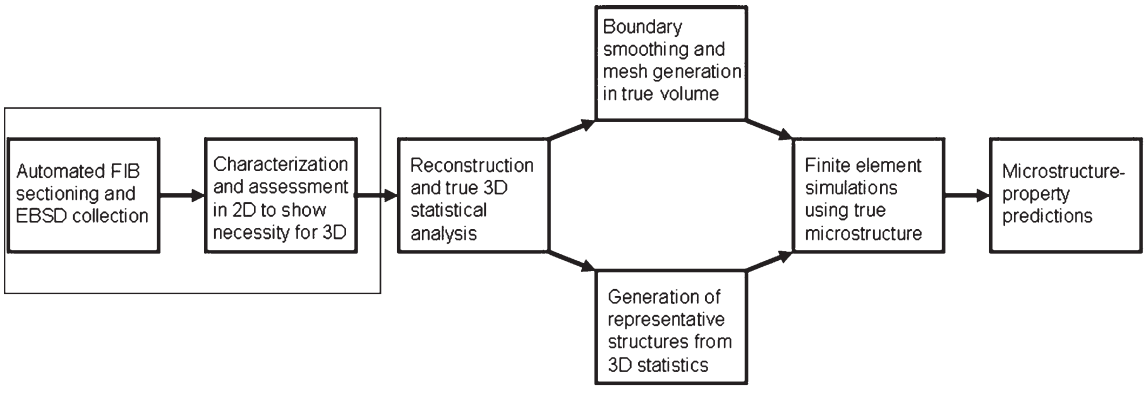

Fig. 1. Flow diagram outlining the 3D data analysis framework. This paper focuses on the data collection techniques and assessment of 2D characterization. It is clear from this work that a "true" 3D analysis is necessary to fully predict critical microstructure–property relationships.

data, as well as a framework for the handling of the 3D data set. This paper discusses a novel procedure for obtaining data from the FIB–SEM, starting from sample preparation to the post-processing of the data. Post-processing of the data is performed using a customized in-house program called "Micro-Imager". This program has the capability for processing the raw data characterization and eventual finite element modeling. Starting from 2D EBSD maps, Micro-Imager automatically defines grains and grain boundary segments, and calculates various statistical features of the microstructure. By utilizing the statistical data for a sequence of 2D EBSD maps from a serial-sectioning experiment, statistical correlations and 3D characteristics of a polycrystalline microstructure can be understood. The focus of the present paper is on developing improved data collection and subsequent statistical analysis techniques. The methods presented in this paper are an integral part of a larger characterization and modeling framework. An outline of this overarching framework is given in Fig. 1. While the ultimate goal of the overall research is to obtain microstructure–property relationships, the present paper only discusses an essential stepping stone in that direction. The results of this study are particularly useful in constructing truly representative material microstructures as input for modeling and simulation programs.

2. Overview of the process, equipment and software used

2.1. The collected data

The data collected in this work consists of 2D crystallographic orientation maps taken from consecutive sections of a serial-sectioning experiment. It is important to understand that the individual maps do not contain direct 3D data. However, the assemblage of the sections can offer quantitative descriptions of the variation in the microstructure over the sectioned volume. Additionally, the 2D orientation maps can be assembled to produce a reconstructed true 3D volume. In this paper, the analysis will focus on the handling of each individual section as well as quantifying the variation between sections. This work is the first step towards 3D reconstruction and characterization of the microstructure.

2.2. Equipment used

Acquiring serial-section data requires specialized equipment to accurately extract functional information from the microstructure. The essential equipment used in this research is:

i. *Dual beam focused ion beam–scanning electron microscope (FIB–SEM):* This microscope is capable of highly localized micro-machining and ion imaging using the FIB column, and non-destructive high-resolution imaging or other analytical methods such as electron backscatter diffraction (EBSD) using the electron column. The FIB can be automated, through the use of control scripts, to section, position, and image the specimen. Precise positioning and alignment of the specimen is performed using the FIB's image recognition capabilities. The FIB system can mill sections with a thickness as low as 50 nm, but because of time constraints a larger thickness of 250 nm was used in this experiment.
ii. *Electron backscattered diffraction (EBSD) system:* The EBSD system used in this work was developed by TSL and is the source of the quantitative orientation information used to automatically delineate grains and grain-boundary segments. The EBSD system, which is also automated in this process, collects crystallographic orientation information across each section, producing a series of 2D orientation maps. The EBSD system can obtain orientation data with a resolution as high as 50 nm, but again time constraints called for a lower resolution of 250 nm in this experiment.

2.3. Software used

Analyzing the serial-sectioning data requires a significant amount of processing and subsequent microstructural measurement. A combination of commercially available programs and in-house developed codes are used to efficiently handle the serial-sectioning data. These are:

i. *Micro-Imager:* Micro-Imager is a special purpose code developed in our laboratory for this work. It processes the orientation information from the EBSD system and automatically defines grains and grain-boundary segments by analyzing discrete changes in local orientation. After Micro-Imager clearly defines the microstructure constituents, it calculates and outputs characterization parameters such as the distribution of grain size, number of neighboring grains, grain orientation, and grain boundary misorientation angle for every 2D section. Table 1 lists the parameters calculated by Micro-Imager and outlines the measurement methods.

Table 1
List of the parameters measured by Micro-Imager

Parameter	2-D measurement	Application	3-D counterpart
Grain area fraction	The number of grid points assigned to a grain plus the approximation error divided by the number of total grid points in the scan.	This parameter can be used to find the area of every grain in the scan. The grain area fraction of each grain is multiplied by the total scan area, giving a distribution of grain sizes.	Grain volume fraction
No. of neighboring grains	As new boundaries are found, they are added to a running list. At the end of boundary detection, it is known how many neighbors each grain has.	This parameter is useful in looking at grain growth characteristics as well as grain-to-grain interactions.	No. of neighboring grains
No. of edges of a grain	The number of line segments needed to complete the boundary of a grain is the number of edges of that grain.	This parameter defines the curvature of the boundary. If the edges equal the neighbors, then the boundary is facetted, but if there are many more edges, the boundary must have more curvature.	No. of faces of a grain (instead of line segments it is plane segments)
Grain perimeter	The length of each line segment is known and added together to determine the perimeter around a grain.	This parameter can be used to determine the total grain-boundary-length-per-area, which can be used to determine grain boundary area per volume through stereology.	Grain surface area
Misorientation	The misorientation is measured for every neighbor of a grain and this is done for every grain.	This parameter is useful to calculate an MODF profile and also is useful in grain-to-grain interactions, stress intensities, and crack nucleation and growth.	Misorientation

Also included are the measurement method, the application of the parameter, and 3-D counterpart.

ii. *IMOD:* IMOD is a commercially available code which consists of a set of image processing tools for tomographic reconstructions [16]. MIDAS, which is a feature of the IMOD program, is used to align the 2D sections collected in the serial-sectioning experiment. MIDAS allows the user to manually determine the best alignment between two consecutive images. Details of the program can be found at [16], and thus the process will not be discussed in this paper.
iii. *Fovea Pro:* Fovea Pro is a suite of image analysis software plug-ins used in conjunction with Adobe PhotoShop. Fovea Pro is used to calculate stereological parameters for comparison and validation with Micro-Imager. In this work, Fovea Pro is used to measure the lineal mean intercept and the grain boundary surface-area-per-volume from each 2D section.

3. Experimental procedure

3.1. Material analyzed

The material selected for analysis in this work is a fine-grained powder metallurgy-processed nickel-based superalloy (IN100). A FIB secondary electron image of the material microstructure can be seen in Fig. 2. The process history of the IN100 sample contained a sub-solvus heat-treatment, which results in a microstructure of γ and γ' grains having secondary γ' precipitates within the γ grains. The thermo-mechanical processing yields relatively equiaxed grains having a fine grain size (~2 to 5 μm average).

The small grain size allows for a large number of grains to be examined during the course of the FIB serial-sectioning experiment. Presently, the sampling volume is practically limited to $50 \times 50 \times 50\,\mu m^3$ due to the time needed to perform the experiment (~4 days). Another distinct advantage was that IN100 formed high "quality" EBSD patterns, which enabled the OIM system to acquire data at its fastest speed.

There are also a number of complications that are encountered when using this material system. The

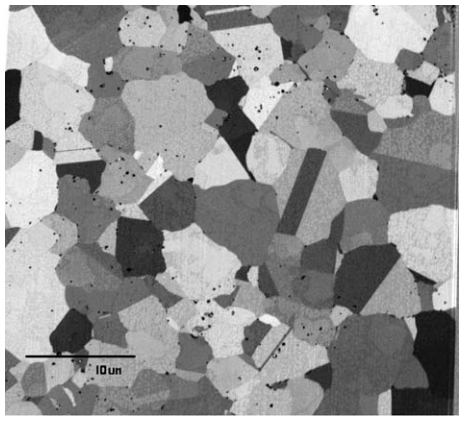

Fig. 2. Microstructure of IN100 Ni-based superalloy shown in a FIB secondary electron image.

extensive twinning and multi-constituent structure present challenges that have been discussed later in this paper. It is important to note that the experimental process developed in this work is theoretically material independent, but issues of grain size, EBSD pattern quality, and microstructure complexity are all factors that will affect the speed and feasibility of the data collection and analysis.

3.2. Specimen fabrication and preparation

The specimen-preparation steps for the IN100 sample are as follows. First, a diamond saw is used to section a small amount of material from a bulk sample, with dimensions of approximately 5 mm × 5 mm × 0.5 mm. The thickness of this section is further reduced by mechanical polishing to roughly 50 μm. Once polished, the sample is mounted on a SEM stub and placed on a 38° pre-tilted sample holder, which is needed to access the necessary tilt angles for the serial-sectioning experiment. The sample is then inserted into a FEI Company Strata Dual Beam 235 FIB–SEM.

Prior to starting the serial-sectioning experiment, the FIB is used to mill a cantilevered "finger" geometry at the edge of the specimen, as shown in Fig. 3. This sample geometry is used to eliminate problems with redeposition of sputtered material during the sectioning experiment, and also to enable EBSD mapping of the serial-sectioned surface. After fabricating the finger geometry, a platinum cap is deposited on the top surface of the finger via a platinum gas-injection source. The DB235 microscope has the capability to locally deposit materials such as platinum and tungsten using precursor gases that react with the ion or electron beam. In these experiments, the platinum cap is used to protect the surface of the sample normal to the ion beam, since the experiments involve a cumulative period of ion imaging which could significantly erode the top surface of the finger. Additionally, the platinum cap tends to improve the fidelity of the serial-sectioning experiment since the smooth surface of the cap helps to eliminate "water-falls"-vertical streaks visible on the cross-sectioned face that can be caused by surface roughness [17]. Surface roughness on the sectioned face can affect the quality of the EBSD pattern and compromise the ability of the EBSD system to properly index the pattern.

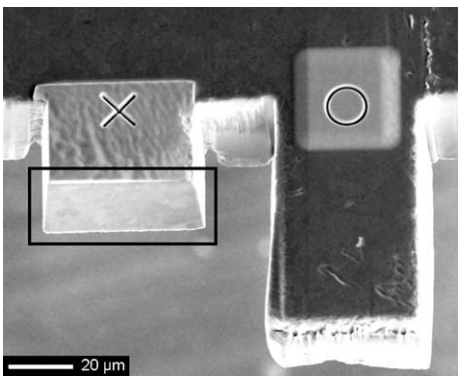

Fig. 3. SEM image of FIB–EBSD sample showing cantilevered "fingers" and the fiducial marking pattern. The finger on the left has undergone sectioning and the finger on the right has been rough-milled and would be smoothed prior to sectioning. The analyzed surface is labeled by the box.

The final step of the sample fabrication process involves FIB-milling fiducial marks into the top surface of the sample. The fiducial marks are used to precisely reposition the sample after moving the microscope stage between serial-sectioning milling and image-analysis positions. This is discussed in the next section. For this experiment, two fiducial patterns (a cross and a circle) are used that are easily distinguished from each other, as seen in Fig. 3.

3.3. Stage rotation and repositioning

The serial-sectioning experiment in the dual-beam FIB–SEM is comprised of moving the sample repeatedly between two microscope stage positions. These positions are the "sectioning" position and the "ion imaging/EBSD analysis" position, as shown in Fig. 4. When the sample is in the sectioning position, the FIB is used to mill a cross-section surface that is normal to the long axis of the finger geometry with a 3000 pA beam. After sectioning, the sample stage is rotated and translated to bring this cross-section face into the ion imaging/EBSD analysis position. For the 38° pre-tilted holder, a rotation of 180° and a tilt 4° is needed to move between the two positions. Once moved, the cross-sectioned surface is at an optimal angle for EBSD analysis (~70° angle of inclination between the electron beam and the normal of the cross-section surface). This stage position also allows for imaging of the same surface with the ion-beam, albeit for smaller ion beam currents (100 pA) than are typically used for cross-section milling.

3.4. Image recognition for precise positioning and alignment

The fiducial marks described previously in Section 3.2 are critical for precise alignment of the sample at

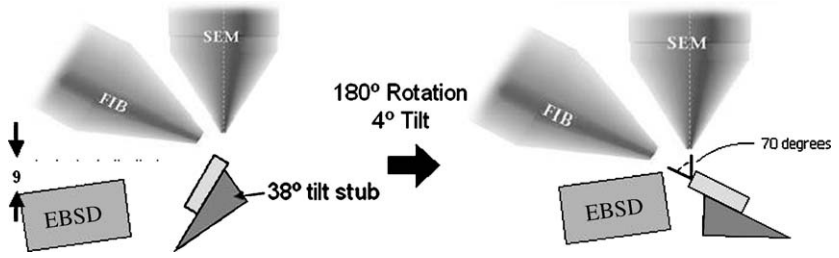

Fig. 4. Schematic of the two-stage positions in the dual-beam microscope for the sectioning and imaging process. The schematic on the left shows the ion-cutting position while the schematic on the right shows the EBSD mapping position.

the two stage positions, as the microscope stage is only accurate to within a few microns when moving between the two stage positions. That level of precision is insufficient for producing serial-sectioning data having sub-micron resolution in the sectioning thickness. However, use of the built-in image-recognition software together with the fiducial marks enables sub-micron precision. The image-recognition procedure is as follows. After the microscope moves the sample to either the "sectioning" or "imaging/EBSD analysis" position, the image-recognition software is used to identify the fiducial mark placed in-line with the finger geometry (see Fig. 3). Furthermore, it uses this mark to accurately place the specimen in the desired location. The image-recognition software is subsequently used to correct for any rotational misalignment. Specifically, the image-recognition software identifies the location of both fiducial marks, and those values are compared to the original values at the start of the serial-sectioning experiment. The rotation of the specimen stage is adjusted such that the misalignment is less than 0.1°. After correcting for rotational alignment, the program corrects for stage drift, i.e. a smaller amount of time-dependent movement following a large repositioning of the stage. Specimen drift is accounted for by putting a time delay in the program, which is followed by another image recognition step. Allowing the stage to settle for approximately 10 to 20 s is found to correct for specimen drift rather well for the imaging conditions used in this experiment.

Lastly, the image recognition software is also used for final placement of the serial-sectioning milling pattern, which defines the location where the FIB sputters material away to create each section. The distance from the fiducial mark to the end of the finger is determined at the beginning of the experiment, and is continually updated by subtracting the value of the section thickness multiplied by the total number of sections. The use of the built-in image recognition abilities of the DB235 ensures a consistent slice thickness for the serial-sectioning experiment. Having a known constant section thickness is an important factor for reconstruction of a 3D volumetric structure from the serial-sectioning data and is one of the distinct advantages of this automated process. Visual examination of the entire series of image data obtained from the experiment suggests that the section thickness is consistent. At present, variability in the serial-sectioning thickness has not been specifically measured.

3.5. Some details of experiment

The experimental data collected for this study comes from a specimen of dimensions 40 μm × 41 μm × 29 μm. The inter-slice thickness for this experiment is 250 nm and the point-to-point spacing in each OIM scan is also 250 nm. Each slice takes approximately 25 min to execute using the following steps: ion milling, sample rotation, ion-image capture, EBSD scan, and sample rotation back to the sectioning position. The entire experiment generated 117 sections that took just over two days of automated serial sectioning to complete. The EBSD or OIM scan takes significant time to perform in the overall process. For an EBSD scan area of 50 μm × 50 μm, each OIM map requires approximately 11 min to collect the crystallographic data, scanning at 58 points-per-second (20 kV, spotsize 6) and using a step-size of 250 nm. Roughly 45% of the time of the experiment is spent collecting the OIM data. The other time-consuming process is FIB milling, as 35% of the time is spent sectioning the sample with a 3000 pA beam current. With increasing acquisition speed of the OIM system and the optimized FIB systems for high-current milling, these experiments can be performed faster and higher resolution data will be available without a significant increase in acquisition time.

4. Data processing and microstructure delineation with Micro-Imager

There are many commercially available software packages for visualizing 3D data. However, these packages are not equipped to automatically segment grains and generally only provide visualization capabilities. The development of the Micro-Imager code is a direct result of the need to process the orientation data and quantify the microstructure. The first objective of the Micro-Imager code is to define the microstructure constituents, such as grains and grain boundaries. Delineation of the microstructure corrects artifacts produced by the EBSD system and clearly defines the microstructure for subsequent quantitative analysis. The second function of Micro-Imager is to provide tools to evaluate statistical characterization parameters for describing the microstructure. This section of the paper will present the methodology used by Micro-Imager to accomplish these objectives.

4.1. Grain segmentation with Micro-Imager

The Micro-Imager program has been developed to create well defined grain boundary contours in 2D from the image data through a series of contiguous line-segment representations. In this module, the grain boundaries are identified as an assemblage of points delineating change in crystallographic orientations. Grain boundaries can have a tortuous topology and many local fluctuations in the orientation maps. Micro-Imager approximates these spatially complex boundaries with line segments by using an error-per-unit-length (EUL) algorithm. This process corrects artifacts like aliasing of grain boundaries that are produced when collecting the EBSD data, as well as defines the grain structure for subsequent mesh generation for computational modeling. The EBSD data collection acquires crystallographic information on a square grid, and the resulting description of the grain boundaries becomes aliased or "stair-stepped". The approximation of grain boundary positions using line segments effectively smoothes these boundary steps by passing a straight line segment through the pixels constituting the boundary. A schematic diagram illustrating the creation of an aliased boundary is shown in Fig. 5.

Boundary detection in Micro-Imager incorporates comparing the Euler-angle values of a given pixel to its four nearest neighbors. A pixel's Euler angles are the set of angles that define its orientation in space in relation to a global coordinate system. A set of three Euler angles, (φ_1, Φ, φ_2), describe the orientation of a pixel and all pixels in a given grain have an essentially equivalent set of Euler angles, within a small tolerance. If the Euler angles of a neighboring pixel do not match that of the reference pixel to within a defined tolerance (4° for this work), the midpoint between the two pixels is tagged as a grain boundary point. The misorientation between the two orientations of the neighboring pixels is calculated to determine if the Euler angles match. The misorientation is defined as

$$\theta = \min\left|\cos^{-1}\left\{\frac{tr(g_A g_B^{-1} O)-1}{2}\right\}\right| \tag{1}$$

where g_A and g_B are the orientation matrices of grain A and B, respectively, expressed as

$$g_i = \begin{pmatrix} \cos\varphi_1\cos\varphi_2 - \sin\varphi_1\sin\varphi_2\cos\Phi & \sin\varphi_1\cos\varphi_2 + \cos\varphi_1\sin\varphi_2\cos\Phi & \sin\varphi_2\sin\Phi \\ -\cos\varphi_1\sin\varphi_2 - \sin\varphi_1\cos\varphi_2\cos\Phi & -\sin\varphi_1\sin\varphi_2 + \cos\varphi_1\cos\varphi_2\cos\Phi & \cos\varphi_2\sin\Phi \\ \sin\varphi_1\sin\Phi & -\cos\varphi_1\sin\Phi & \cos\Phi \end{pmatrix}$$

The angles φ_1, Φ, φ_2 are the Euler angles of grain i, and O is the crystal symmetry operator for the crystal structure. Considering that there are 24 identical rotation operations in cubic symmetry, the misorientation of the two lattices can be described by 24 different symmetrically equivalent rotations. The minimum rotation angle is chosen as the misorientation angle.

This process is completed for every pixel of a given image. Once every boundary point is defined, special boundary points that three or more grains share (triple points) are located. The initial approximation of the grain-boundary positions is simply the segments defined by connection of these special (triple) points.

Micro-Imager refines the representation of the grain boundaries using a figure of merit called the error-per-unit-length. The error-per-unit-length is defined as the area enclosed between the line segment connecting the special points (**AB** in Fig. 6) and the line segments connecting all the points that have been identified as the

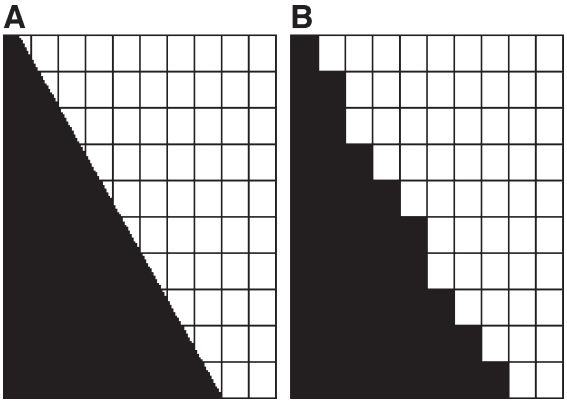

Fig. 5. Schematic displaying the aliasing scheme of a smooth curve: (A) a straight boundary between the dark and light regions, where fractions of pixels are filled; (B) the same boundary with full pixels filled or empty. The stepped nature of the originally smooth line is a result of aliasing.

boundary between the grains, normalized by the length of the line segment **AB**. From the schematic in Fig. 6, this error is expressed as

$$\text{Error-per-unit-length} = \frac{\int_{A}^{B} [t(x) - a(x)]\,dx}{\int_{A}^{B} dx} \tag{2}$$

where $t(x)$ corresponds to points on the grain boundary delineated by orientation change, and $a(x)$ corresponds to points on the initial segment joining the endpoints **A** and **B**. The delineated real boundary is not smooth and hence $t(x)$ is not a smooth function. The integral in the numerator of Eq. (2) is calculated by adding discrete rectangular areas in the histogram.

In Micro-Imager, the user defines a threshold value for the error-per-unit-length. If the error-per-unit-length is higher than the threshold value, the single line segment is divided into two segments having the same bounding special points as the initial segment's endpoints. These two line segments also have a common endpoint on a previously defined boundary pixel, which is shown in Fig. 6B. This procedure is repeated for all line segments until the error-per-unit-length for each of these segments is below the threshold value. A small value for the error-per-unit-length threshold results in segmented boundaries that more closely approximate the actual data, but a threshold approaching zero does not simplify the microstructure. Similarly, a higher threshold value produces a more simplified structure, but it is important to examine whether this process oversimplifies the microstructure and creates artificial or erroneous features.

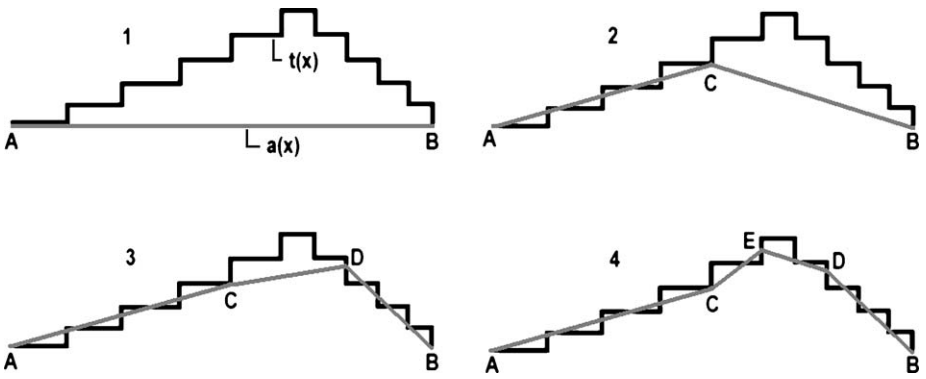

Fig. 6. Schematic showing the evolution of the grain boundary approximation in Micro-Imager. The dark boundary connection labeled $t(x)$ represents the true grain boundary shape and the lighter line segment(s) labeled $a(x)$ represent the approximated boundaries.

Once a satisfactory network of segments is produced, the grains bounded by these segments are used to calculate statistical grain-structure data.

4.2. Measurement of microstructural parameters by Micro-Imager

Once a representative microstructural section from FIB-based serial sectioning has been processed by Micro-Imager, 2D statistical information about the grain morphology can be generated. In the initial phase of this work, five parameters were selected for measurement. These characteristic parameters are plotted for 2D sections and compared with other sections to determine the variation in the sectioning direction. 3D parameters can be calculated using stereological rules [18]. A list of these five parameters and related information is given in Table 1.

5. Results for a typical material grain structure

The grain structure of the IN100 sample is shown in the four images of Fig. 7. The first image is a grain map produced by an OIM scan, the second is the grain map approximation calculated by Micro-Imager, the third is an FIB secondary electron image taken at 7500×, and the fourth is a skeletonized image created by Micro-Imager which is used for the stereological calculations by Fovea Pro. Note that the images in Fig. 7 are of the same area, and the region shown is 40 μm × 41 μm in size. The microstructure of IN100 presents both advantages and complications to this experimental technique. The advantages, as discussed previously, include small grain size, high-quality EBSD patterns, and relatively simple grain morphology. Some of the complications that arise inherently due to the material are the presence of twins and a multi-constituent structure. One issue associated with defining grains is the question of whether to consider

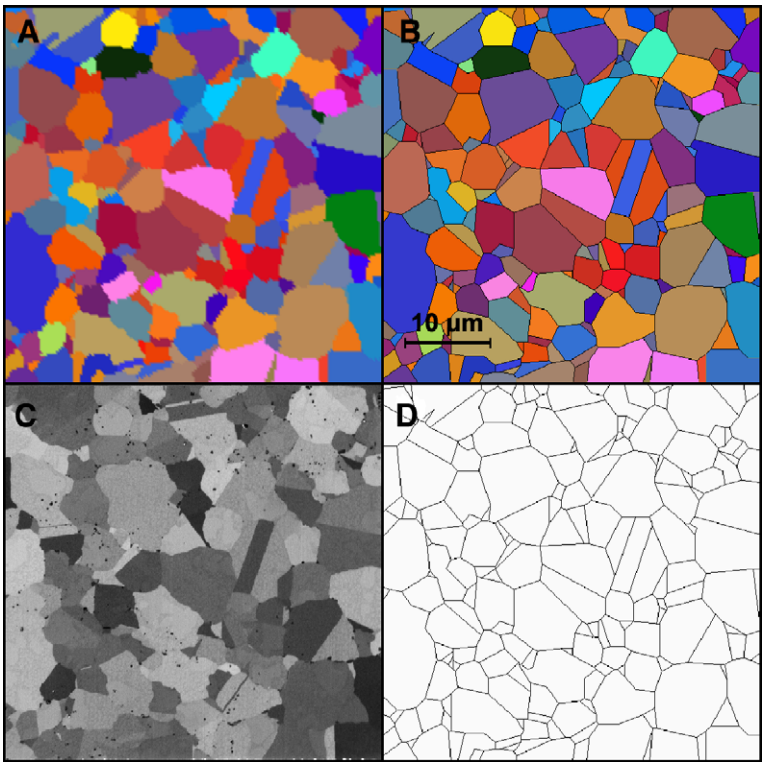

Fig. 7. Microstructure of IN100 Ni-based superalloy, (A) grain map from EBSD scan, with pixel size approximately 250 nm; (B) grain map after grain approximation by Micro-Imager; (C) FIB secondary electron image; and (D) binary image of the grain boundaries as created by Micro-Imager for improved stereology measurements (compare with ion image seen in (C)).

twins as individual grains or to group them with the surrounding grain. For this study, twin boundaries are treated the same as every other grain boundary. The multi-constituent structure presents another complication. The γ and primary γ′ grains cannot be differentiated by the OIM system because the EBSD patterns are virtually identical for the two phases. As a result, all of the grains are considered as a single phase. Additionally, the carbides present in the structure are smaller than the resolution of the EBSD system and thus do not produce clear EBSD patterns. It is the intention to couple additional information available from the ion images to differentiate the primary γ′ grains and locate carbides.

6. Quantitative characterization and statistical analysis

Quantitative analysis of microstructure is performed on the 2D sections to accomplish a number of objectives. The first objective of the quantitative analysis is to validate and compare Micro-Imager's measurements with stereological measurements made by Fovea Pro. Comparison of direct measurements of the microstructural morphology with stereological measurements displays areas where Micro-Imager can make improvements in microstructure characterization. After comparison and validation, the measurements are analyzed to create a quantitative description of the different characterization parameters measured. The final objective in this analysis is to quantify the variation in the consecutive sections, both in the average and extreme values of the distributions. The analysis of variation displays the need for true 3D data.

6.1. Micro-Imager analysis versus stereological methods

Stereology is the science of the geometrical relationships between a structure that exists in three dimensions and the images of that structure that are fundamentally two-dimensional [18]. Stereological formulations are commonly used to determine microstructural parameters such as grain size, grain boundary surface-area-per-volume, and the volume fraction from 2D images. To validate the accuracy of Micro-Imager calculations, measurements of two microstructural parameters, viz. grain area and grain boundary surface-area-per-volume, from Micro-Imager are compared with those predicted by conventional stereological methods. The measurement of grain area using Micro-Imager is straightforward. The area of each grain is simply calculated from the number of pixels assigned to that grain multiplied by the area per pixel. Note that this calculation also includes the fractional area for pixels which are assigned to grain boundaries. The stereological measurement of lineal mean intercept is performed using Adobe PhotoShop with the image analysis software plug-in toolkit Fovea Pro.

Fig. 8A shows a comparison of the average grain area determined by Micro-Imager and by Fovea Pro for each 2D section. To calculate the grain area using the lineal mean intercept method, the grains are considered to be spherical, i.e. the grain area is assumed to be equal to the area of a circle having a diameter equal to the lineal mean intercept. For circles of measured diameter D, the lineal mean intercept $\overline{l}$ is given as:

$$\overline{l} = \left(\frac{\pi}{4}\right) D. \tag{3}$$

There are two curves for the grain area calculated by Fovea Pro. The lower curve is the area calculated by directly considering the lineal mean intercept as the diameter of a circular grain. The other curve is the area calculated by considering the lineal mean intercept as the diameter of a circular grain, but it also includes a corrective multiplicative factor accounting for the probability of intersection through the equatorial plane of the circular grains in a 2D image. The derivation of this multiplicative factor is discussed in Thompson [19] along with additional factors associated with mean intercept calculations.

Fig. 8B shows a comparison of the surface-area-per-volume. Micro-Imager calculates this value by summing the length of all the grain boundary segments for a given grain and dividing this length by the area of the grain, i.e.

$$\left(\text{Boundary length per unit area in 2D}\right)_i = \frac{1}{A_1} \sum_{j=1}^{n} L_{ij} \tag{4}$$

where A_i is the area of the ith grain and L_{ij} is the length of the boundary segment(s) between grains i and its neighbor j, which is summed over all the n neighbors of the grain i. The stereological relation of the boundary length per unit area to the boundary surface area per unit volume is presented in Russ and Dehoff [18] as

$$S_{\mathrm{V}} = \frac{4}{\pi} L_{\mathrm{A}} \tag{5}$$

where S_{V} is the boundary surface area per unit volume and L_{A} is the boundary-length-per-area, calculated by

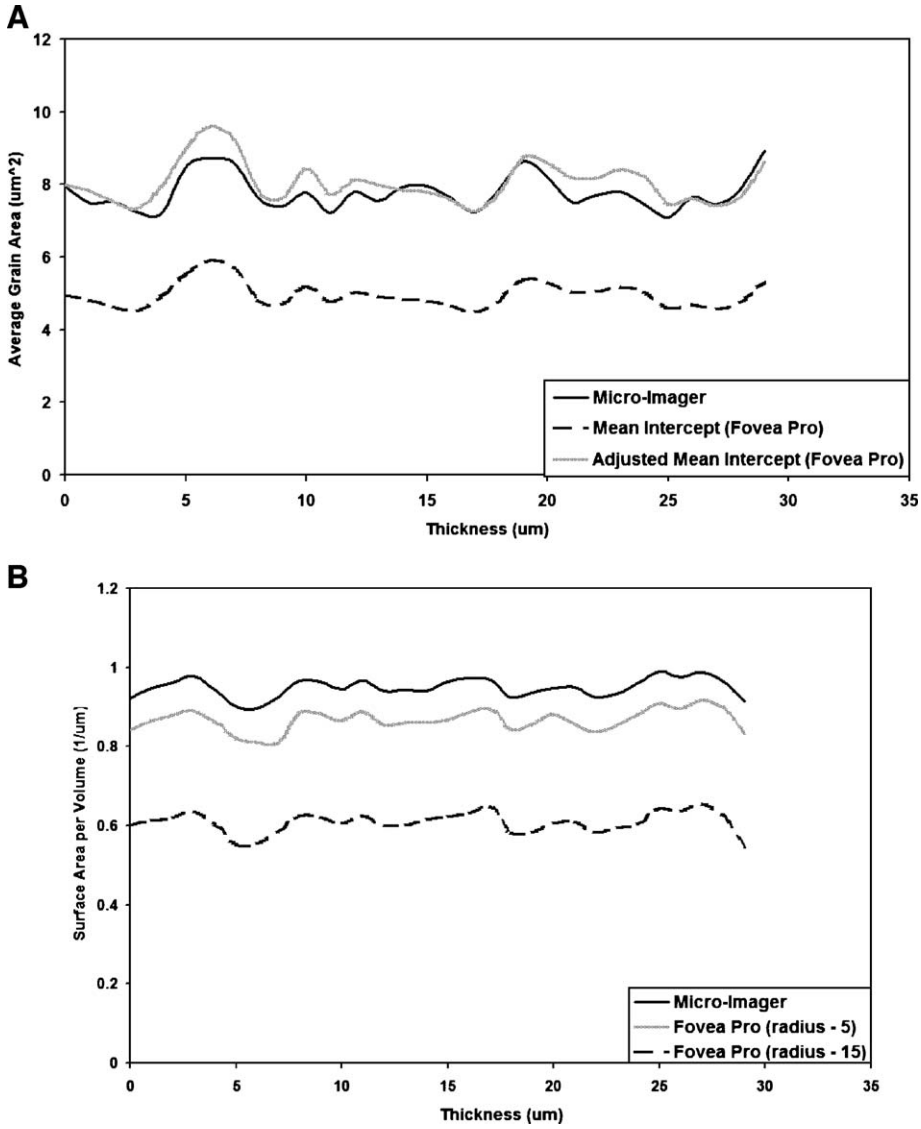

Fig. 8. Comparison of parameter measurements from Micro-Imager and Fovea Pro. The *x*-axis (thickness) corresponds to the position through the depth of the material from which the sections are collected: (A) average value of the grain area, and (B) average value of the grain boundary surface area per unit volume.

Eq. (4). The measurement of the same parameter by Fovea Pro is calculated by counting intersections of cycloids with grain boundaries and is affected by the radius of the cycloids. As the radius approaches zero, the value converges to that measured by Micro-Imager. It is seen in Fig. 8B that the measurements from Fovea Pro converge toward the measurement by Micro-Imager. This example displays an advantage of using Micro-Imager, since some grain structure parameters can be calculated in a manner that is not sensitive to measurement method, unlike some stereological techniques.

6.2. Probability density functions

In addition to calculating the mean values of selected grain structure parameters, some of these parameters are plotted and fitted to determine probability density functions (PDFs), which provide a more complete characterization of the feature distribution. Fig. 9 shows PDFs for grain diameter, misorientation angle, number of neighboring grains, number of grain boundary edges, grain perimeter, and grain area. It is important to note that while continuing development of Micro-Imager seeks to

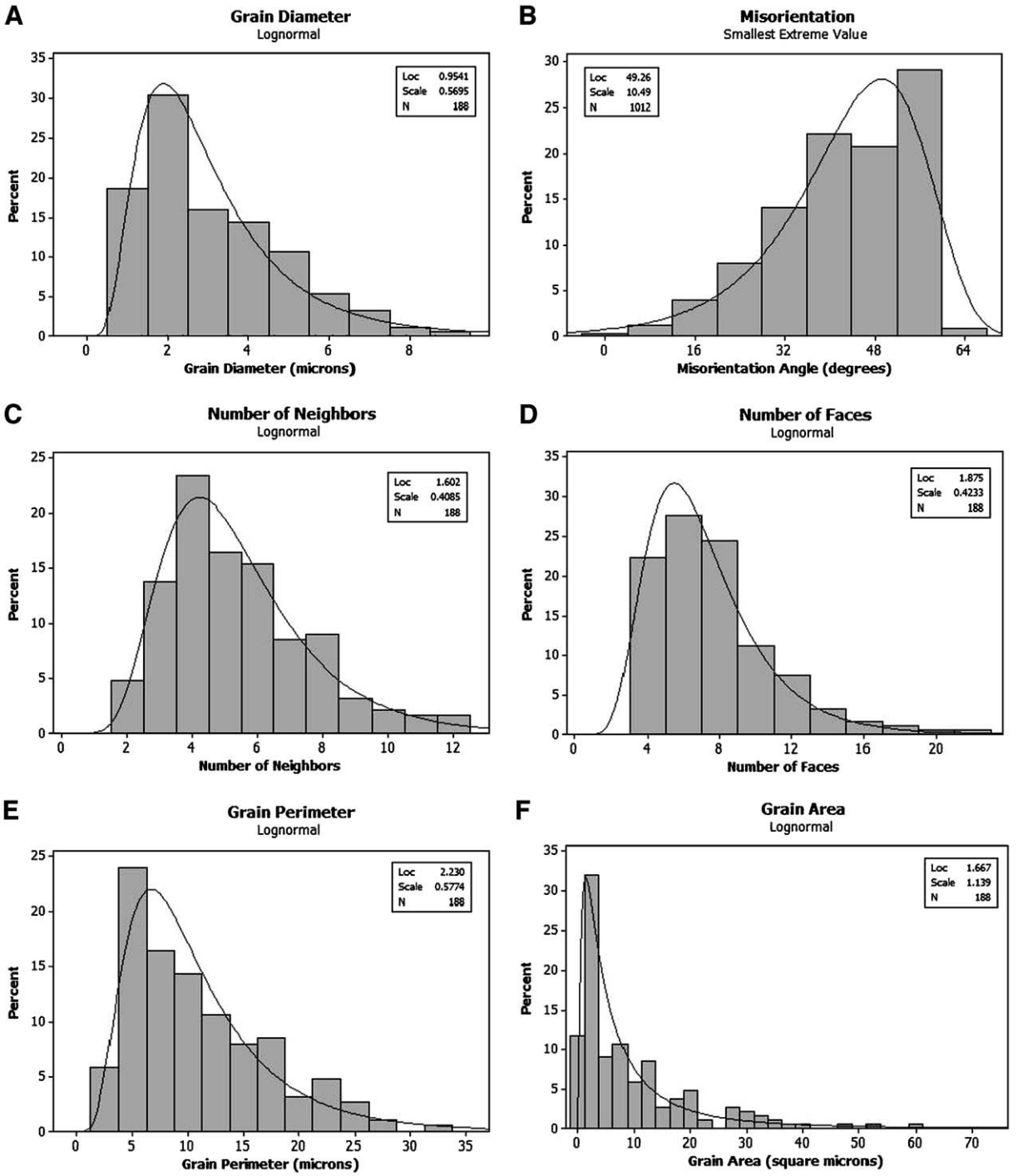

Fig. 9. Probability density functions and data histograms generated by Micro-Imager from a single 2D section: (A) grain diameter, (B) misorientation angle, (C) number of nearest neighbors, (D) number of grain boundary edges, (E) grain perimeter, and (F) grain area. The value of grain diameter in (A) is calculated as the diameter of a circle having the same grain area as in (F).

calculate PDFs from 3D reconstructions of the serial-sectioning data, Fig. 9 is generated from a single 2-D slice. Almost all of the parameters shown in Figs. 9 and 10 are best fit by log-normal curves, except for the misorientation distribution, which appears to be best fit by a smallest-extreme-value curve.

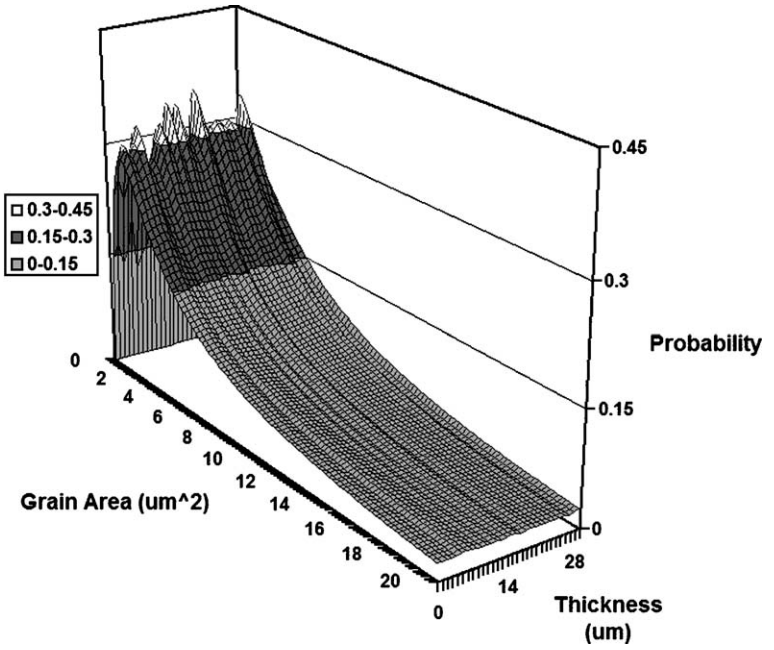

Fig. 10. Probability density functions of grain area for the entire serial sectioning experiment, shown collectively as a surface plot in 3D to highlight variation from section-to-section. The PDFs were only extended to 20 μm^2, as the probability is relatively constant at larger values.

6.3. Parameter variation through sectioning depth

Fig. 10 shows a 3D surface plot that is constructed from the series of individual PDFs from every slice in the serial-sectioning experiment. This plot does not completely substitute for a PDF constructed from a 3D reconstruction. However, the benefit of examining the data in this manner is that changes in the PDFs are easily compared over the sampled volume. If the PDFs vary markedly through the thickness, then one 2D section is clearly not sufficient to describe a particular microstructural feature, and such occurrences are revealed by such plots. One problem that arises when examining PDF plots is that the tails of the distribution are smoothed out, which can be observed in Figs. 10 and 11. Fig. 11 is similar to Fig. 10, but rather than examining

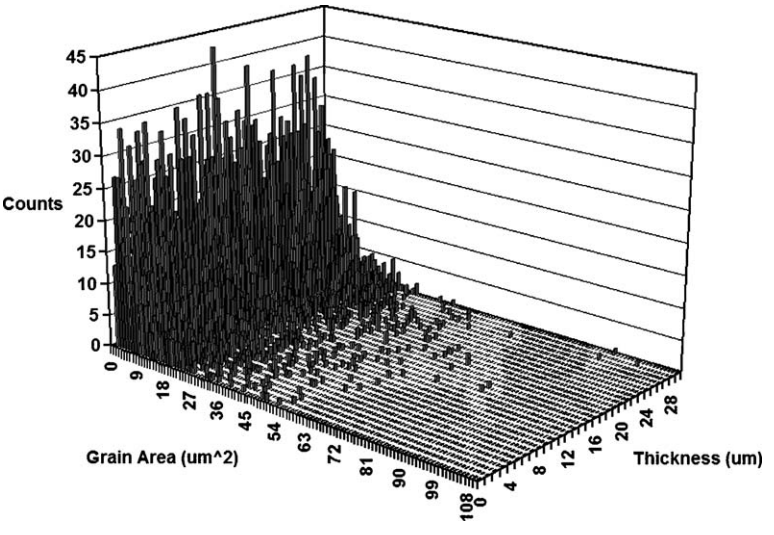

Fig. 11. 3D plot of the binned grain area histograms from individual sections stacked together to show variation as a function of serial-sectioning depth. This figure shows how the maximum grain area can vary markedly from section-to-section.

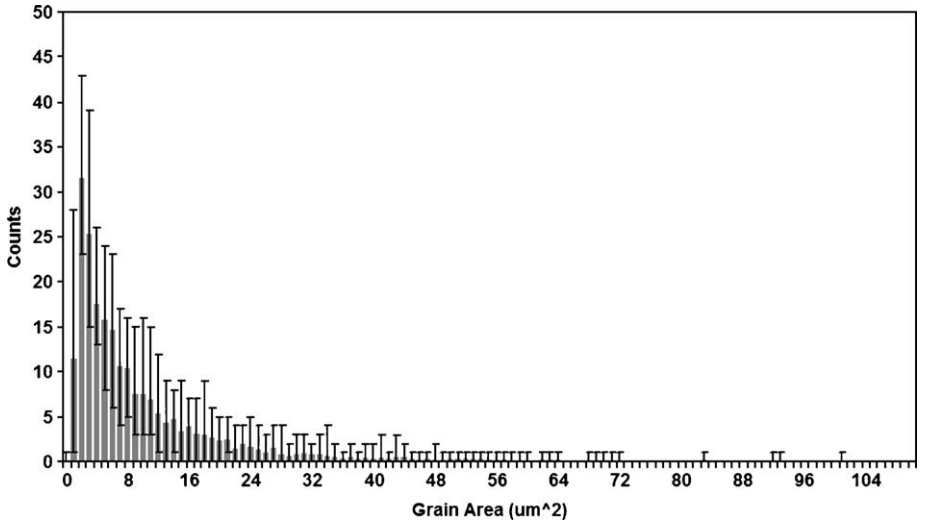

Fig. 12. Histogram of grain area constructed from the averaged bin values for each size range for all of the sections. The error bars show the maximum and minimum values for each size throughout the entire data set.

the series of PDFs as a 3D surface plot, the actual measured histograms of grain area are shown in 3D. The binned data of Fig. 11 clearly shows significant variation in the extreme (maximum) values of the grain-area distribution, from one section to the next.

Additional applications of the characterization methods are shown in Figs. 12 and 13. In Fig. 12, a histogram of the "average" grain area is plotted, by taking the average value for each bin size as calculated over all of the 2D sections in the data set. The error bars in this plot denote the maximum and minimum values for each bin. This figure demonstrates that there is a significant variation in the distribution of grain sizes over the 2D image set, even for sizes which are at or near the mean value. Lastly, Fig. 13 shows a plot which tracks the average grain area and the maximum grain area on every slice. In this figure, one can easily observe that the average grain area appears essentially constant for every slice, but there is a noticeable variation in the maximum (this is also observed in Fig. 11). When taken as a whole, the data analyzed further demonstrates the potential need for more detailed microstructural analysis than simply calculating the average value of a parameter. Often, the average value for a particular microstructural

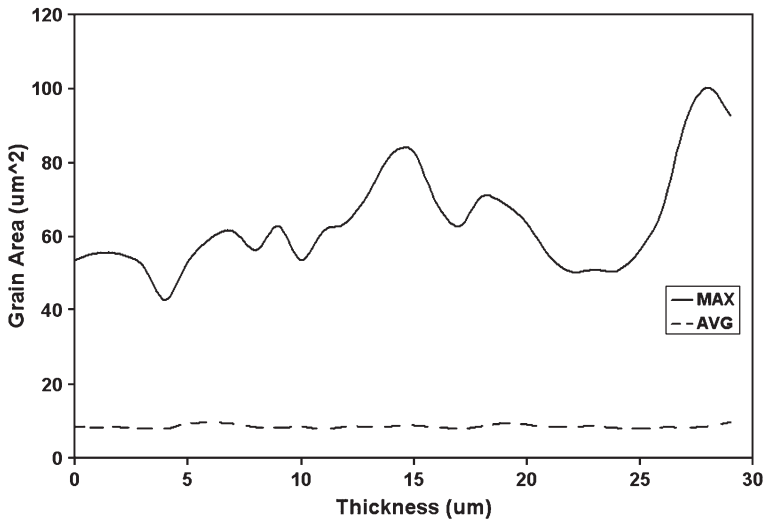

Fig. 13. Plot showing the values for average grain area and the maximum single grain area for each slice. Note that there is relatively little change in the average grain area from slice-to-slice, whereas there is significant variation in the maximum single grain area from slice-to-slice.

feature appears approximately constant from one slice to the next, but the feature can vary markedly in its extreme values. If only the average value of a feature is needed for a property model, then a single section of sufficient size may be adequate. However, if knowledge of the extreme values of a microstructural feature is needed as in determination of fatigue and fracture properties, then it is likely that the information provided by only one or two sections of the material cannot be used to describe the feature. Furthermore, there are some parameters which can only be calculated from 3D microstructural information [2]. This is an area of future research in this effort.

7. Conclusions

This paper introduces both experimental and computational procedures that enable new quantification analysis of grain structure. This work is a first step towards a fully automated process that will both collect 3D microstructural information via serial sectioning and provide quantitative measurements of property-controlling microstructural features. This paper presents a summary of the representation and analysis methodology as it currently exists, which is comprised of characterizing individual slices of the serial-sectioning data using a 2D analysis. Although the characterization methodology is not based on a true 3D analysis, this work has clearly demonstrated some shortcomings in traditional 2D analysis methods, especially with regards to characterizing extreme values. Future work will include improving both the fidelity and range of data types accessible through the serial-sectioning methodology, and expand upon the representation and analysis methods into 3D. A 3D reconstruction of the material microstructure by stacking 2D data and characteristics is near completion, and will be reported in a future paper.

Acknowledgements

The authors acknowledge support from the Materials and Manufacturing Directorate of the Air Force Research Laboratory, in particular M. A. G. and S. G. through contract # F33615-01-2-5225. The authors would also like to thank Joe Ullmer, Stuart Wright, Damian Dingley, and Paul Scutts of TSL Inc, and Robert Wheeler and Robert Kerns of the Microstructural Characterization Facility for helping incorporate the remote-trigger OIM system into the serial sectioning methodology.

References

[1] Samuels LE. Metallographic polishing by mechanical methods. Metals Park, OH: American Society for Metals; 1982.
[2] DeHoff RT. Quantitative serial sectioning analysis: preview. J Microsc 1983;131:259–63.
[3] Ghosh S, Moorthy S. Particle fracture simulation in non-uniform microstructures of metal–matrix composites. Acta Mater 1998;46:965–82.
[4] Kurzydlowski KJ, Ralph B, Bucki JJ, Garbacz A. The grain boundary character distribution effect on the flow stress of polycrystals. Mater Sci Eng, A Struct Mater: Prop Microstruct Process 1995;205:127–32.
[5] Kurzydlowski KJ. On the dependence of the flow stress on the grain size distribution in polycrystals. Scr Metall 1990; 24:879–84.
[6] Li M, Ghosh S, Richmond O, Weiland H, Rouns TN. Three dimensional characterization and modeling of particle reinforced MMCs: Part I. Quantitative description of microstructural morphology. Mater Sci Eng, A Struct Mater: Prop Microstruct Process 1999;A265:153–73.
[7] Li M, Ghosh S, Richmond O, Weiland H, Rouns TN. Three dimensional characterization and modeling of particle reinforced MMCs: Part II. Damage characterization. Mater Sci Eng, A Struct Mater: Prop Microstruct Process 1999;A266:221–40.
[8] Sakamoto T, Cheng Z, Takahasi M, Owari M, Nihei Y. Development of an ion and electron dual focused beam apparatus for three-dimensional microanalysis. Jpn J Appl Phys 1998; 37:2051–6.
[9] Dunn DN, Hull R. Reconstruction of three-dimensional chemistry and geometry using focused ion beam microscopy. Appl Phys Lett 1999;75:3414–6.
[10] Phaneuf MW, Li J. Proc Microsc Microanal 2000;6:524–5.
[11] Inkson BJ, Steer T, Möbus G, Wagner GT. Subsurface nanoindentation deformation of Cu–Al multilayers mapped in 3D by focused ion beam microscopy. J Microsc 2001;201:256–69.
[12] Inkson BJ, Mulvihill M, Möbus G. 3D determination of grain shape in a FeAl-based nanocomposite by 3D FIB tomography. Scr Mater 2001;45:753–8.
[13] Lee E, Williams R, Viswanathan GB, Banerjee R, Fraser HL. 3D materials characterization using dual-beam FIB/SEM techniques. Proc Microsc Microanal 2004;10:1128–9.
[14] Williams R, Bhattacharyya D, Viswanathan GB, Banerjee R, Fraser HL. Application of FIB-tomography to the study of microstructures in titanium alloys. Proc Microsc Microanal 2004;10:1178–9.
[15] Claves SR, Bandar AR, Misiolek WZ, Michael JR. Three-dimensional (3D) reconstruction of AlFeSi intermetallic particles in 6XXX aluminum alloys using focused ion beam. Proc Microsc Microanal 2004;10:1138–9.
[16] http://bio3d.colorado.edu/imod.
[17] Orloff J, Swanson L, Utlaut M. High resolution focused ion beams: FIB and applications. New York: Kluwer Academic/ Plenum; 2002.
[18] Russ JC, Dehoff RT. Practical stereology. New York: Kluwer Academic/Plenum; 2000.
[19] Thompson AW. Calculation of true volume grain diameter. Metallography 1972;5:366–9.